DESIGN FOR ADDITIVE MANUFACTURING OF KINEMATIC PAIRS

Shrey Pareek*, Vaibhav Sharma*, and Rahul Rai*

*Design Analytics Research and Technology (DART) Lab,
Department of Mechanical and Aerospace Engineering,
University at Buffalo-SUNY, Buffalo-NY, 14260

REVIEWED

Abstract

While additive manufacturing processes are better suited for fabrication of parts with complex geometries, they face serious challenges whilst fabricating parts that require relative motion with respect to each other. The primary challenge in additive manufacturing of mechanisms is preventing the mating parts from bonding with each other during the fabrication process. In this paper the authors investigate design and additive fabrication of kinematic pairs that can move relative to each other. The paper outlines fabrication of kinematic pairs based on optimal clearance value for three basic lower order kinematic pairs, viz. revolute pair, prismatic pair, and cylindrical pair. Using empirical testing functional relationships between extractive force and clearance, and between moment and clearance have been developed. These functional relationships can be used by users to fabricate kinematic pairs using FDM based 3D printing processes. The efficacy of the proposed approach is demonstrated on 3D printed kinematic pairs and experimental validation studies.

Introduction

Additive manufacturing holds the unquestioned advantage over conventional manufacturing techniques when it comes to fabrication of parts with complex geometries. However, additive manufacturing (Fused Deposition Modeling in particular) encounters serious challenges whilst fabricating parts that require relative motion with respect to each other. Generally such models require that each part be produced separately and then assembled together. However, due to inherent inaccuracies of 3D printing these assemblies seldom function correctly. For instance, inaccurate circularity of a 3D printed shaft may prevent its smooth movement inside the hub. This problem can be eliminated through allocation of appropriate clearance. An appropriate clearance is one that allows for unobstructed functioning of the assembly while avoiding unwanted motions/vibrations such as wobbling in case of a shaft and hub.

Current 3-D printing technologies require that the user make amends to the original CAD model to account for appropriate clearance. However, this clearance is user defined. This leads to sub-optimal clearance specification. Sub-optimal clearances cause problems in proper functioning of the mechanism. Additionally, sub-optimal clearance specification necessitates multiple design iterations to identify optimal clearance in an ad-hoc manner. Multiple design iterations make the entire process entire process time consuming. The outlined method in this paper provides structured and effective way of determining optimal clearance for fabrication of 3D printed kinematic pairs. The suggested method is also fast, robust, and eliminates ad-hoc design iterations.

Revolute and prismatic pairs have rotational and sliding relationships w.r.t. each other respectively. A cylindrical pair exhibits both rotary and sliding relationships. The paper provides the optimal clearance value based on the user's needs for three basic lower order kinematic pairs, viz. revolute pair, prismatic pair, and cylindrical pair (Figure 1). For the purpose of this paper we focus on clearance and interference fits only [1]. Tight fit is not considered as the proposed method allows the designers to use the 3D printed part directly i.e. no finishing operations are carried out on the 3D printed part and 3D printed kinematic parts can be used 'as is'. For the purpose of this study a Fused Deposition Modeling (FDM) MakerBot Replicator 2X® is used as the 3D printing device. The results can be extended to other additive manufacturing techniques and 3D printing devices using suitable adjustments.

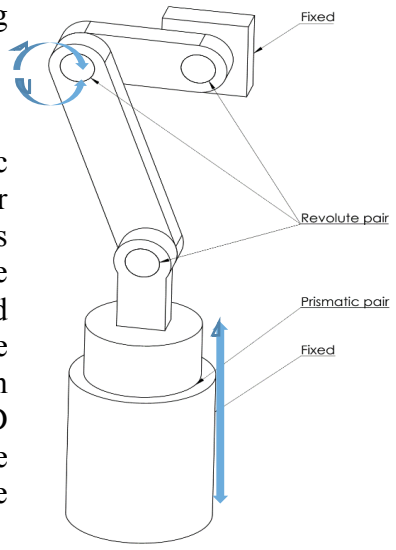

Figure 1 - Schematic representation of Kinematic Pairs.

Literature Review

The following section reviews previous work done in the field of additive manufacturing of assemblies and studies focused on understanding the relationship between surface roughness and limits, fits, and tolerances. Although the focus of the majority of the existing work is on interference fits, they provide us with vital information that can be extrapolated for clearance fits as well.

Preventing the mating parts from bonding with each other during the fabrication process is a major concern in additive manufacturing. For example, the CAD model of a piston-cylinder assembly ignores the clearance gap and the diameters of both the piston and cylinder is considered the same. This equal diameter is read as a single entity by the slicing algorithm, leading to fusion of the two parts. There are various methods implemented to counter this problem; *Lipson et al.* [2] successfully reproduced fully functional and preassembled kinematic models of Reuleaux's kinematic pairs.

Clearance between parts is responsible for determining the type of fit [2]. Studies have shown that in case of clearance fits, contact area increases with increase in load. Also the magnitude of circumferential stress depends on whether or not friction is considered [3]. Joint clearance is a critical deciding factor if the model is to exhibit the preferred movement. A lower clearance results in a tight fit restricting movement and difficulty in removing the support structure or powder from the gap and in some cases a water jet is used to remove the material [4]. To avoid tight fits *Chen et al.* suggested filleting or chamfering to ensure that there is enough contact area and no instability [5]. High clearance yields the joint unstable [6, 7]. Hence optimum joint clearance should be incorporated to get a functional joint. *Chen et al.* developed a drum pin joint by hit and trial method to minimize the joint clearance to the optimum level. This clearance also increased the joint strength simultaneously [6].

The effect of clearance in joint stiffness has also been studied [3]. It has also been shown that the fits in SLA depend heavily on surface roughness [8]. *Yang et al.* [9] study the effect of surface roughness on interference fit between a shaft and a hub. They compare the surface roughness with assembly pressure and fit. Additionally, they also outline a numerical formulation for loss of tightening. Using the numerical formulation they conduct experiments to show that surface texture greatly influences strength of fit. According to there numerical formulation extractive strength is a function of the friction coefficient and nominal contact pressure. The influence of surface finish on interference fits is further studied by *Ramachandran et al*. [10]. Although they study the load carrying capacity of fits w.r.t. the surface roughness, their approach and experimental investigations are of importance. The above observations serve as building blocks towards the formulation of the method proposed in this paper. Details related to these building blocks are outlined in the subsequent sections. It should be noted that the effect of stresses on the clearance are beyond the scope of this study.

In case of Stereo Lithography (SLA), inserts of different materials are used [11]. Another technique is the use of a second release material placed in the gaps between the movable parts. This material is later etched, dissolved, melted or blown away [9]. Removal of support material might lead to a change in alignment of mating parts [9]. In cases where no support structures are used instead of inserts, the clearance should be adjusted to ensure that the structure does not crash on removal of support structures [12].

Further, most 3D models do not specify how their parts move or interact with each other. This leads to difficulty in visualization of the final part. For example a rolling shaft-hub pair may be treated as a sliding couple. *N. Mitra et al.* [12] developed a semi-automatic technique that determines the motion of parts and their causal relationships based on their geometry. This technique requires user assistance for successful analysis of CAD models. We propose a simpler technique that determines the correct clearance on the basis of conditions pertinent to each type of motion. It is assumed that parts rotate about a symmetric axis and/or translate along translation symmetry directions. These assumptions help in identification of translational or rotational axes and their degrees of freedom. If a part (P) remains unchanged under some transformation T_j i.e. T_j (P) = P, it is symmetric about that transformation axis [11].

J Cali et al. [13] developed an automated technique that fits a 3D model into printable joints. They also focused on the aesthetic aspects of the final printed material. Adjustments were made in the model for it to exhibit internal friction. Our study ignores the aesthetic aspects and the internal friction of the model, and focuses mainly on functioning of the mechanisms. Most of the aforementioned studies focus on use of SLA for additive manufacturing of mechanisms, whereas we use FDM as the premise for this study.

Methodology

Using computer simulations and experimental analysis we deduce functional relationships between clearance and extractive force, and clearance and moment required to rotate a rotational pair. These simulations and experiments are explained in the current section. During assembly all CAD packages require the designer to define the relative motion between components. Based on the relations defined in the assembly model the empirically deduced

functional relationships may be used to select the relevant conditions pertaining to each type of kinematic pair.

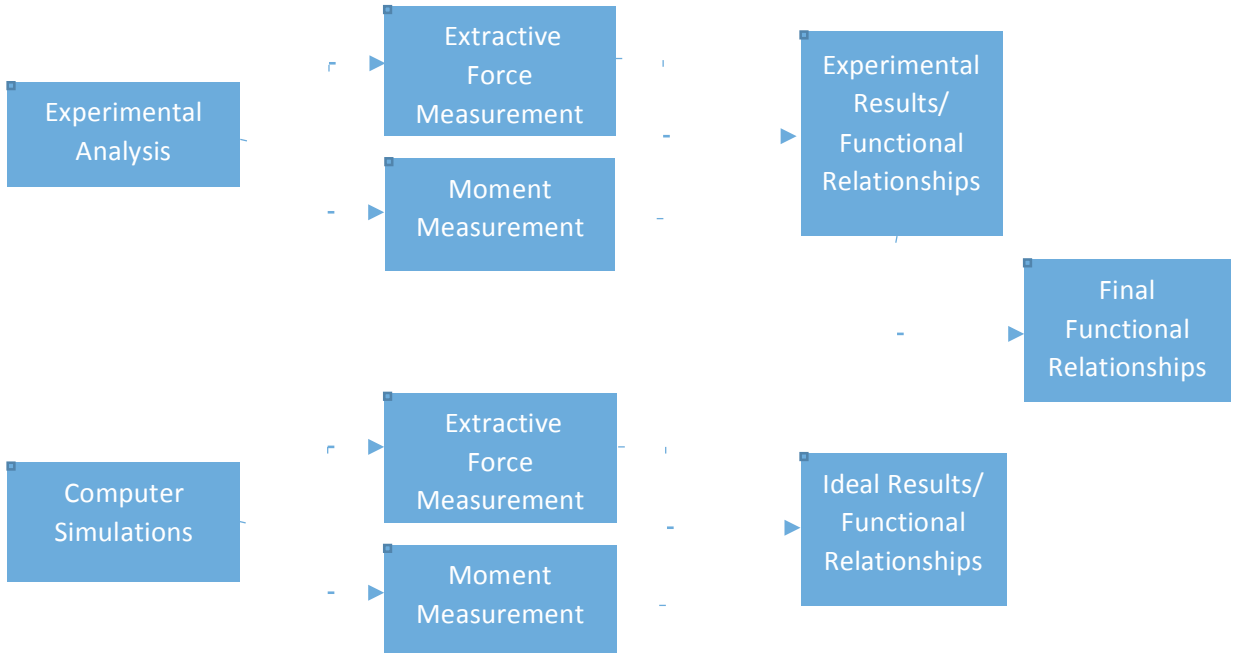

Figure 2 - Schematic Representation of the proposed methodology

Figure 2 provides a basic process flow of the overall methodology. The study comprises of experimental analysis and computer simulations to study the effect of change in clearance on extractive force and moment required to rotate a rotational pair (revolute pair and cylindrical pair). Extractive force is defined as the minimum axial load that is sufficient to displace a linear pair (prismatic pair and cylindrical pair). Results obtained from the experimental analysis and computer simulations (ideal results) are analyzed separately and w.r.t. each other to arrive at the final functional relationships.

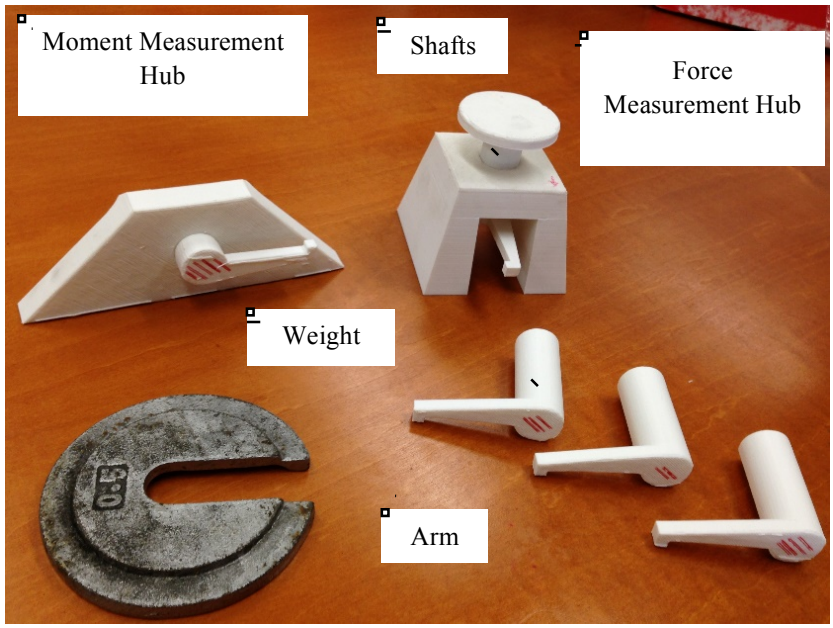

Figure 3 – Components used for Experimentation

Experiment

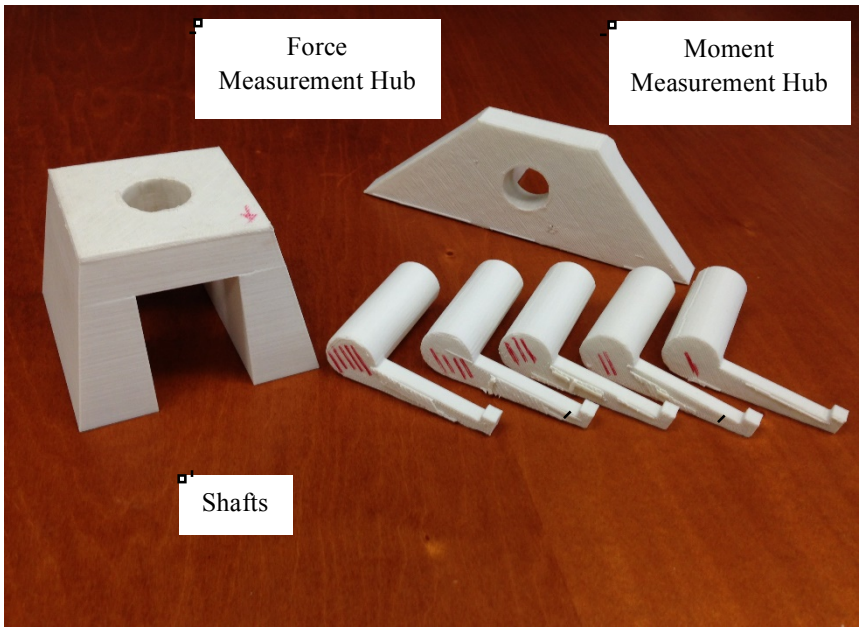

Figure 4 – Disassembled Hubs and Shafts

Using Acrylonitrile Butadiene Styrene (ABS) as the base material and MakerBot Replicator 2X® as the FDM printer experimental analysis is carried out. To imitate the three kinematic pairs (prismatic, revolute and cylindrical) a shaft and hub arrangement is used. The diameter of the hub is kept constant at 20 mm and the shaft diameter is varied from 19.20 mm to 19.75 mm in increments of 0.05 mm. Diameters above 19.75 mm are ignored as they require chamfering operations of the end faces in order to insert the shaft into the hub. Since our process targets at using the 3D printed parts directly without any machining operations, samples with diameter greater than 19.75 mm are disregarded. The length of the shaft and hub are fixed at 50mm and 15mm respectively. An arm of length 47.5 mm is also provided at one end of the shafts in order to apply the moment (Figure 1). A total of 60 shaft samples (five samples for each diameter; 19.20 mm, 19.25 mm, 19.30 mm, 19.35 mm, 19.40 mm, 19.45 mm, 19.50 mm, 19.55 mm, 19.60 mm, 19.65 mm, 19.70 mm, and 19.75mm) are printed using standard settings (Table 1). Rafts and support materials are used and the samples are printed vertically in order to maintain the circularity of the shaft and hub. Two different hub samples, one for force and the other for moment measurements are printed. The hub samples double up as fixtures for the experiment (Figure 3).

Table 1 – Printing Parameters

Nozzle Movement Speed	Print Speed	Nozzle Temperature	Bed Temperature	Layer Height
150 mm/s	90 mm/s	220^{o}C	150^{o}C	0.20 mm

Extractive Force

In order to calculate the extractive force required to achieve linear motion, the shaft is housed vertically in the force measurement hub and is loaded axially from the top (Figure 5). Extractive force for each diameter is taken as that minimum load which is sufficient to overcome the static friction between the hub and the shaft. Standard weights are used to obtain a rough

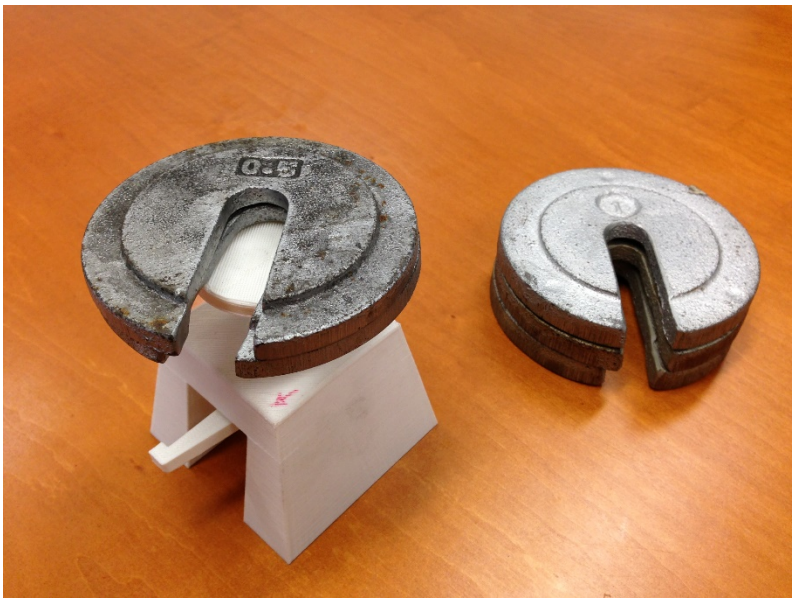

Figure 5 – Extractive Force Measurement

estimate of the load required and water filled beakers are used to obtain finer results. All samples are arranged in the same orientation while carrying out the experiment. As stated previously five samples for each diameter are used. Self-weight of each shaft is also considered in the analysis. All measurements are carried out in grams and are accurate up to two decimal places.

Figure 6 – Moment Measurement

Moment

The moment required to overcome the static friction in the circumferential direction for each sample is measured. In this case the shaft is housed horizontally inside the moment hub and load is applied at the end of the arm (Figure 6). The orientation of the samples is kept the same and standard weights and water filled bags are used for rough and fine load measurements respectively.

Computer Simulations

In order to gain an insight on the how the results obtained from the above experimental analysis differ from the ideal results, computer simulations of the above experiments were carried out using Finite Element Analysis (ANSYS®). Similar to the experimental setting, extractive force and moment variation w.r.t change in diameter of the shaft (clearance) are carried out. During FEA simulations, the dimension of the hub is kept at a constant diameter of 20mm and the diameter of the shaft is varied from 19 mm to 21mm over 100 data points. These data points are randomly generated by the software program. For each value of the shaft diameter, the shaft is given a longitudinal displacement (0.1 mm) in case of the sliding and cylindrical pair, and an angular displacement (1^{o}) in case of the revolute and cylindrical pair. Variation of extractive force/moment required on the shaft w.r.t. the varying diameter (clearance) is calculated and plotted. Figure 7 depicts the specimen used for the simulations. Simulations of

force and moments transmission across the shaft and hub are also carried out. Figure 8 demonstrates force transmission simulation for a 19.982 mm shaft.

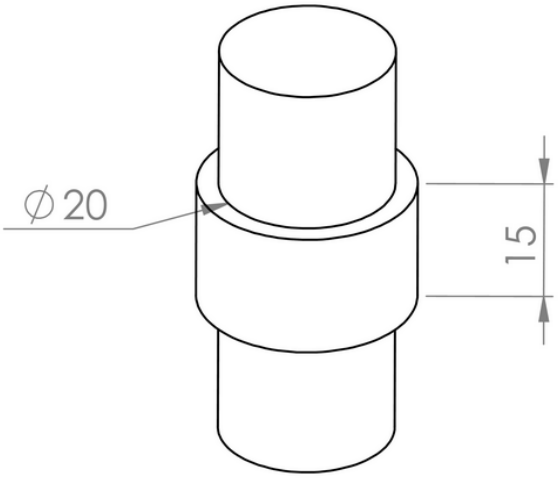

Figure 7 - Specimen

Experimental and Computational Analysis

Experimental Analysis

Once the force and moment data points are obtained, they are averaged over the five samples at each diameter (clearance) value. These averaged points are then plotted against the clearance and polynomial regression analysis [14] is carried out in order to obtain the best fitting curve. Figure 9 shows the graph of Extractive Force v/s Clearance for the experimented data points. The blue circles denote the averaged data points obtained by the experimental analysis and the black line is the best fitting cubic curve. A very high goodness-of-fit value (R^2) of 0.9789 assures that the generated function is a good estimate of the relation between extractive force and clearance. Similarly Figure 10 shows the variation of moment as a function of clearance. The results are summarized in Table 2.

Computer Simulations

Figures 11 and 12 show the plots generated for the Extractive Force and Moment respectively using computer simulations. It should be noted here that 100 different values of clearance were used. Similar to the previous case curve fitting is carried out and the functions are approximated. The results are summarized in Table 3.

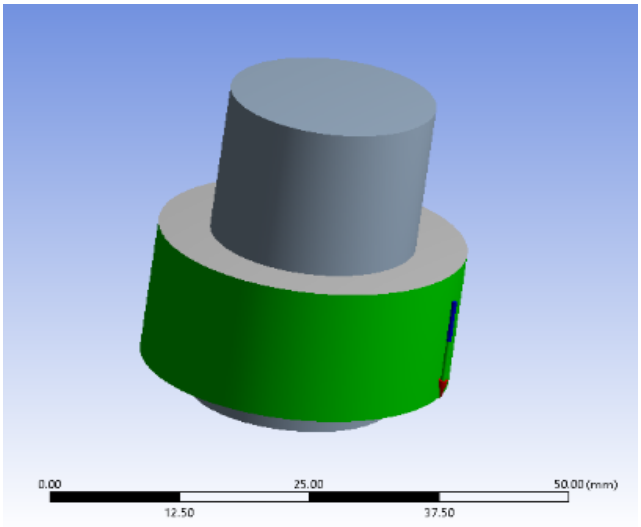

Figure 8 - Force Transmission Simulation

Table 2 - Experimental Analysis Results

Condition	Degree	Constraints	Goodness-of-Fit (R^2)
Extractive Force	3	$y = -715.38x^3 + 1428.8x^2 - 956.37x + 216.06$	0.9789
Moment	2	$y = 1287.1x^2 - 2479.2x + 1181.1$	0.9794

Table 3 - Computer Simulation Results

Condition	Degree	Constraints	Goodness-of-Fit (R^2)
Extractive Force	3	$y = -259557x^3 + 120347x^2 - 15706x + 475.29$	0.9865
Moment	3	$y = -3E+06x^3 + 1E+06x^2 - 161257x + 5215.8$	0.9871

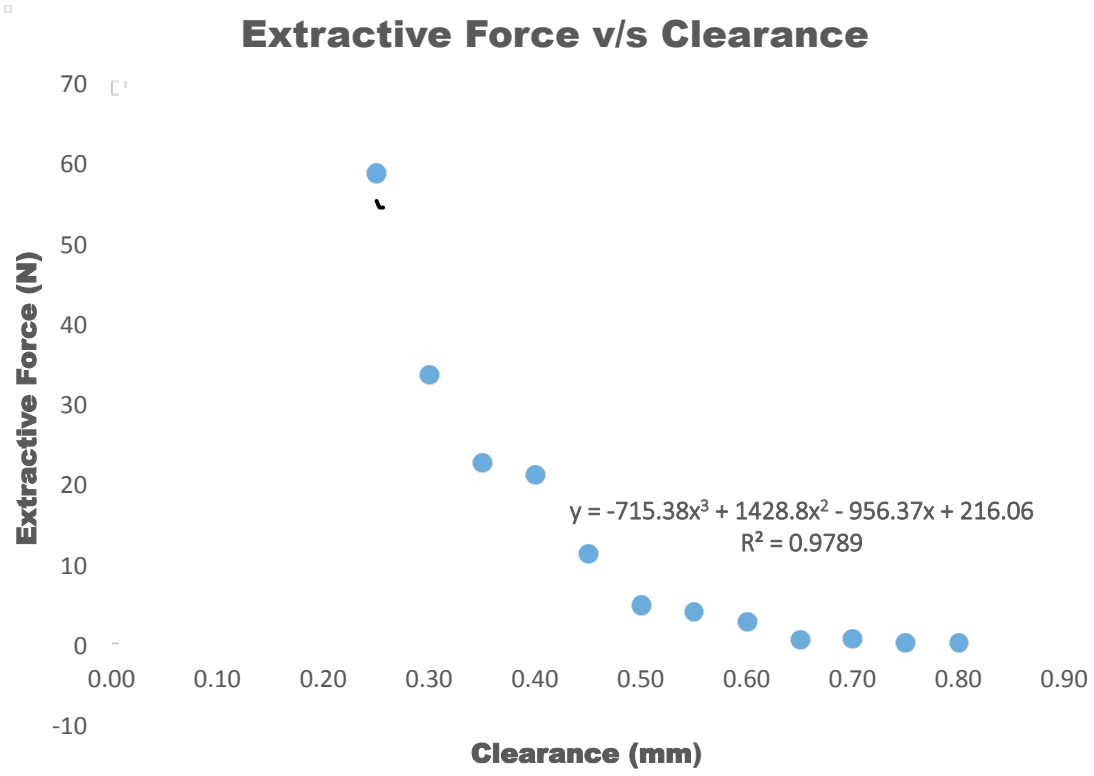

Figure 9 – Extractive Force Variation (Experimental)

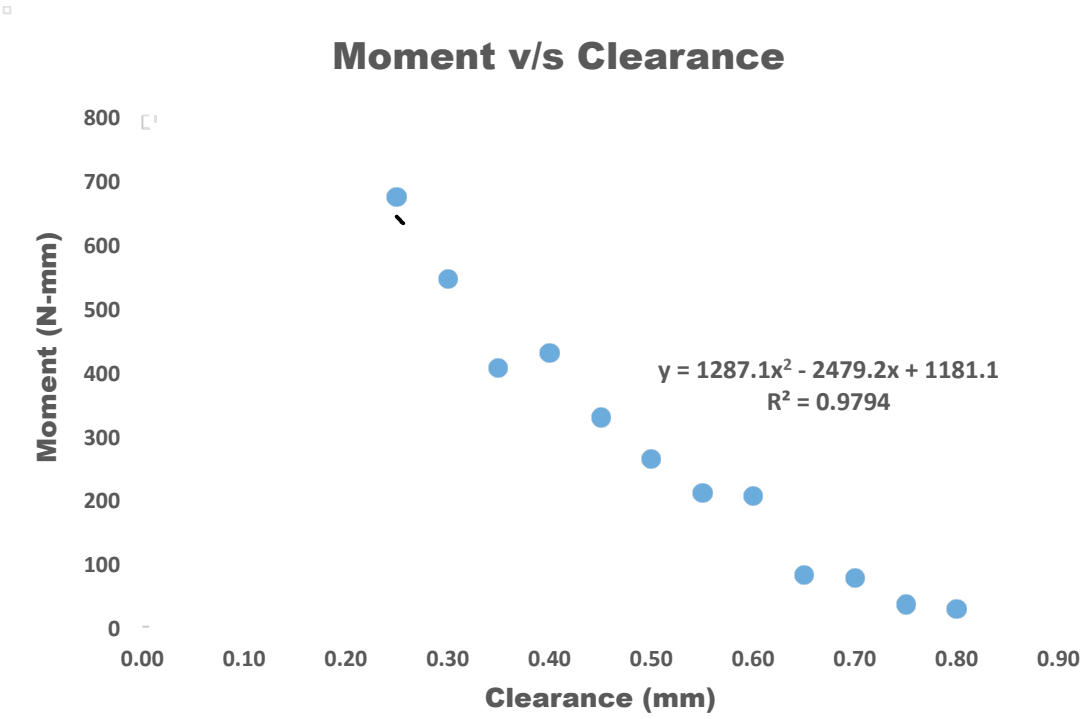

Figure 10 – Moment Variation (Experimental)

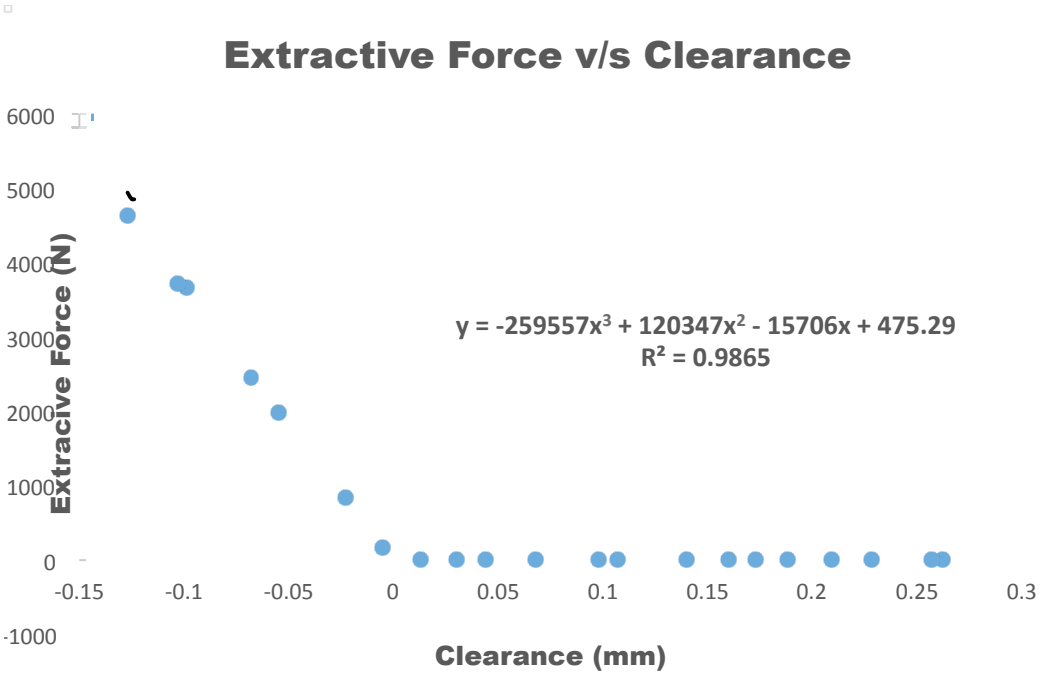

Figure 11 – Extractive Force Variation (Simulations)

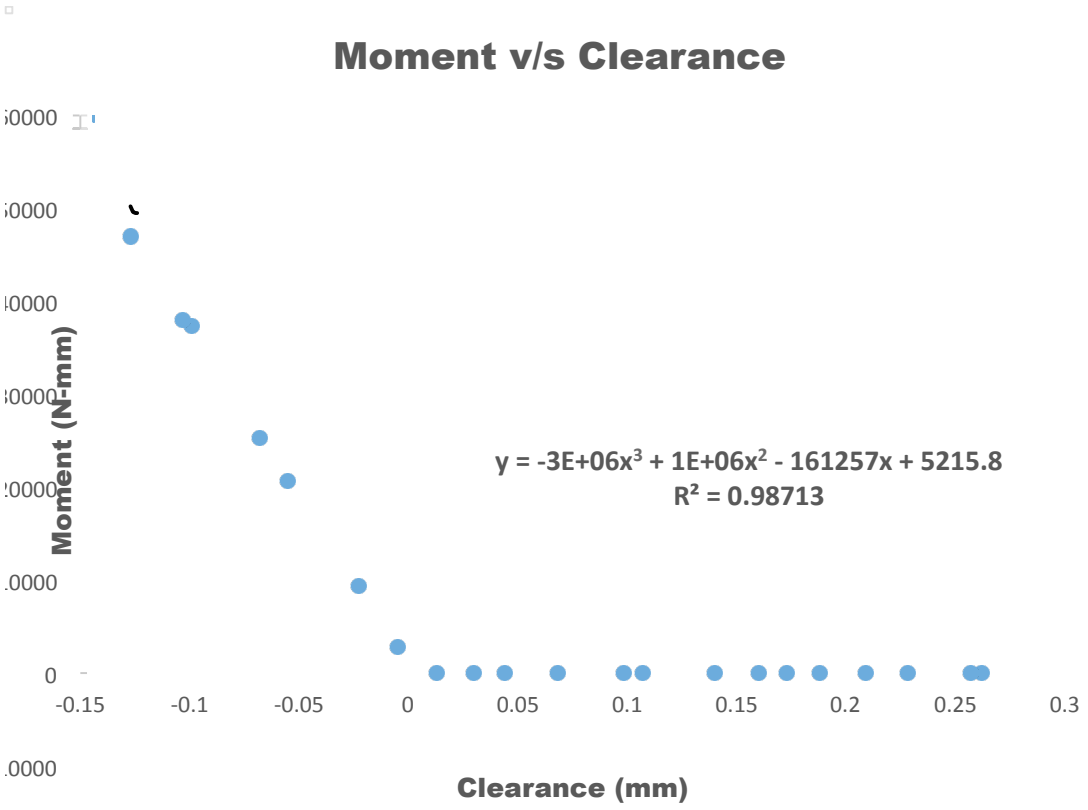

Figure 12 – Moment Variation (Simulations)

From the graphs obtained (Figure 9-12), it is observed that both the Extractive Force and Moment decrease with an increase in clearance. This observation complies with the common knowledge about fits and their relationship with these forces. Careful observation of the results obtained from computer simulations (Figure 11-12) show that as the clearance is decreased the value of force (and moment) is constant at 0 N (N-mm) initially. A sudden increase in force and moment values is observed below clearances of 0.05 mm. These results suggest an optimal clearance within the range of 0 to 0.05 mm. However realization of a clearance of this small magnitude is not possible with the current 3D printer being employed. The computer simulations are thus deemed as ideal results and are overpowered by the experimental results, which are discussed in the next paragraph. Further, results obtained from force transmission simulations (Figure 8) suggest 100% force transmission and show no (zero) energy loss between the shaft and the hub. These results assert the differences between ideal (computer simulation) results and experimental results. There is always some loss in transmitted force (energy loss) in any kinematic pair. Energy loss is not captured accurately by computer simulations. The above observations augment the ineffectiveness of computer simulations and hence simulation results were discarded and only experimental results were used for deriving functional relationships.

Graphs obtained from experimental analysis (Figures 9-10), are more useful for practical purposes. The difference in experimental and simulation results can be attributed to the

inaccuracies of 3D printing. Phenomenon such as warping or vibrations leads to inaccurate geometries (eccentricity of the shaft and hub in this case).

Results

The final functional relationships are obtained using empirical analysis and are shown below. In the following equations, y denotes the Extractive Force/Moment (Equation 1 and 2) and x denotes the optimal clearance corresponding to that force/moment value.

$$y = -715.38x^3 + 1428.8x^2 - 956.37x + 216.06 \quad \textbf{(1)}\ \text{(Extractive Force v/s Clearance)}$$

$$y = 1287.1x^2 - 2479.2x + 1181.1 \quad \textbf{(2)}\ \text{(Moment v/s Clearance)}$$

Extractive force and moment conditions are the active conditions for a sliding pair and a revolute pair respectively. In case of a cylindrical pair both conditions are active. This pair is treated as a special case wherein the user selects one condition as the active one. For instance, if the user chooses the moment condition to be the active one, equation 2 is used to obtain the optimal clearance, which can then be used in equation 1 to obtain the corresponding extractive force. The relationship between moment and extractive force pertaining to a cylindrical pair can be summarized using Figure 13 and Equation 3.

$$y = 108.3x^{0.4627} \quad \textbf{(3)}\ \text{(Moment v/s Extractive Force)}$$

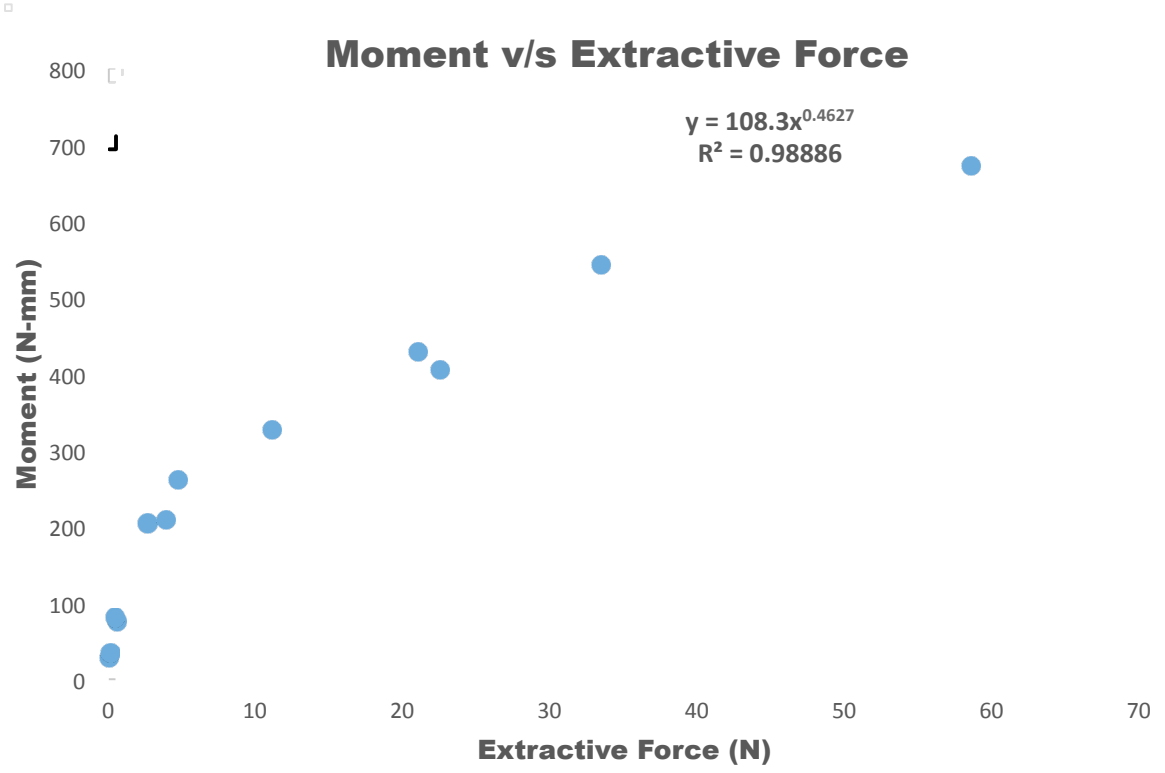

Figure 13 – Moment v/s Extractive Force for Cylindrical Pair Design

Validation

In order to show the utility of the proposed method, we outline the following examples.

Example 1 – Prismatic Pair

Assuming for a particular prismatic pair (shaft-hub pair in this case), an extractive force of 30 N is required. In order to obtain the optimal clearance for this particular application, the Extractive Force – Clearance relationship (equation 1) is used. Using this relation the optimal clearance is determined as 0.331 mm.

To validate the usefulness of this result, a shaft-hub pair with clearance 0.331 mm is 3D printed using the printing parameters listed in Table 1. It should be noted that for validation purpose, we used a different 3D printer but of the same make (MakerBot Replicator 2X ®). For the sake of consistency the hub is kept at a diameter of 20 mm and the shaft diameter is taken as 19.669 mm (clearance 0.331 mm). Extractive force measurements as described in Section 3.1.1 was carried out. The analysis yielded an extractive force value of 26.82 N as opposed to the initial assumption of 30N. This slight deviation in the observed value can be attributed to inherent inaccuracies of 3D printing process.

Example 2 – Revolute Pair

Assuming a moment requirement of 200 N-mm and using equation 2 (Moment-Clearance Relation), the optimal clearance value is determined as 0.556 mm. Similar to example 1, this value is validated using a moment experiment on a 3D printed shaft-hub pair with clearance 0.556 mm (Section 3.2.2). The observed moment value was found to be 232.69 N-mm. This value differs from the original assumed value of 200 N-mm. This variation is acceptable and can be termed as the error of the proposed method.

Example 3 – Cylindrical Pair

A cylindrical pair requires linear as well as rotary motion. For this particular scenario we use the prismatic pair from Example 1 and add a rotary relation to it. As described in section 5, we select either the extractive force condition or the moment condition as the active one. In this case, selecting extractive force as the active condition with a value of 30 N, we determine the corresponding moment value as using equation 3 as 522.50 N-mm. Knowing the experimental extractive force value as 26.82 N from example 1, the moment value is measured using the method employed in example 2. The observed moment value for this case is 473.82 N-mm. Again a deviation from the calculated value (522.50 N-mm) is observed.

As mentioned earlier the deviations observed in the above cases can be attributed to the inaccuracies and inconsistencies of 3D printing. Since the measured values are averaged over the five samples at each diameter, the functional relationships are bound to be erroneous. Despite these inherent errors, the above examples demonstrate that our method has practical utility.

Conclusion and Future Work

The primary challenge in additive manufacturing of kinematic linkages is preventing the mating parts from bonding with each other during the fabrication process. This problem can be eliminated through allocation of appropriate clearance. The paper addresses the challenge of 3D printing of movable linkages and proposes a novel and robust technique that optimizes the clearance between these linkages. Using experimental analysis functional relationships between extractive force and clearance; and between moment and clearance was developed. The clearances obtained from the deduced functional relationships were shown to be optimal for clearance and interference fits. This optimal clearance assures proper functioning of the 3D printed joints and avoids unnecessary motion/vibration.

The slight error in the method can be attributed to inherent inaccuracies of the 3D printing process and errors from experimental estimations (averaging values over five samples at each diameter/clearance). The presented approach could be used for most FDM printers and can be easily extended to other dimensions and additive manufacturing processes. For the purpose of this study, effects due to internal friction and stresses have been ignored. Incorporation of these factors into the study may lead to more accurate results. The study has focused on lower order kinematic pairs (sliding, prismatic and cylindrical) and needs to be extended to higher order linkages (ball and socket joint, universal joint) in order to enable 3D printing of variety of kinematic linkages. The study has focused on clearance as the sole design variable. Increasing the number of variables by varying the printing parameters (nozzle, velocity, bed temperature, and material) can make the method more robust. Studies exploring the relationship between surface roughness and extractive force/moment could be particularly beneficial for 3D printing parts with clearance fits.

References

[1] *Mechanical engineer's reference book*. Vol. 9. Butterworth Heinemann, 1998.

[2] Lipson, Hod, Francis C. Moon, Jimmy Hai, and Carlo Paventi. "3-D printing the history of mechanisms." *Journal of Mechanical Design 127*, no. 5 (2005): 1029-1033.

[3] McCarthy, M. A., V. P. Lawlor, W. F. Stanley, and C. T. McCarthy. "Bolt-hole clearance effects and strength criteria in single-bolt, single-lap, composite bolted joints." *Composites science and technology* 62, no. 10 (2002): 1415-1431.

[4] Changhui, Song, Yang Yongqiang, Ye Ziheng, and Wang Di. "Digital design and direct manufacturing of non-assembly mechanisms by selective laser melting." In *Assembly and Manufacturing (ISAM), 2013 IEEE International Symposium on*, pp. 142-144. IEEE, 2013.

[5] Chen, Yonghua, and Chen Zhezheng. "Joint analysis in rapid fabrication of non-assembly mechanisms." *Rapid Prototyping Journal* 17, no. 6 (2011): 408-417.

[6] Chen, Yonghua, and Jianan Lu. "Minimize joint clearance in rapid fabrication of non-assembly mechanisms." *International Journal of Computer Integrated Manufacturing* 24, no. 8 (2011): 726-734.

[7] Yang, Yongqiang, Di Wang, Xubin Su, and Yonghua Chen. "Design and rapid fabrication of non-assembly mechanisms." In *Manufacturing Automation (ICMA), 2010 International Conference on*, pp. 61-63. IEEE, 2010.

[8] Kataria, Alok, and David W. Rosen. "Building around inserts: methods for fabricating complex devices in stereolithography." *Rapid Prototyping Journal* 7, no. 5 (2001): 253-262.

[9] Yang, Gong-Ming, J. C. Coquille, Jean François Fontaine, and M. Lambertin. "Influence of roughness on characteristics of tight interference fit of a shaft and a hub." *International journal of solids and structures* 38, no. 42 (2001): 7691-7701.

[10] Ramachandran, R. V., and V. Radhakrishnan. "Influence of surface finish on interference fits." *International Journal of Production Research* 12, no. 6 (1974): 705-719.

[11] Binnard, Mike, and Mark R. Cutkosky. "Design by Composition for Layered Manufacturing*." *Journal of Mechanical Design* 122, no. 1 (2000): 91-101.

[12] Mitra, Niloy J., Yong-Liang Yang, Dong-Ming Yan, Wilmot Li, and Maneesh Agrawala. "Illustrating how mechanical assemblies work." *ACM Transactions on Graphics (TOG)* 29, no. 4 (2010): 58.

[13] Calì, Jacques, Dan A. Calian, Cristina Amati, Rebecca Kleinberger, Anthony Steed, Jan Kautz, and Tim Weyrich. "3D-printing of non-assembly, articulated models." *ACM Transactions on Graphics (TOG)* 31, no. 6 (2012): 130.

[14] Draper, Norman Richard, and Harry Smith. "Applied regression analysis 2nd ed." (1981).